Available online at www.CivileJournal.org

Civil Engineering Journal

(E-ISSN: 2476-3055; ISSN: 2676-6957)

Vol. 10, No. 12, December, 2024

Comparison of Multi-Objective Metaheuristics for Discrete Optimization of Steel Trusses Using Direct Analysis

Trung-Hieu Tran [1], Quoc-Anh Vu [1], Viet-Hung Truong [2], Ngoc-Thang Nguyen [2*]

[1] Faculty of Civil Engineering, Hanoi Architectural University, Hanoi, Viet Nam.

[2] Faculty of Civil Engineering, Thuyloi University, 175 Tay Son, Dong Da, Hanoi 100000, Viet Nam.

Received 11 August 2024; Revised 07 November 2024; Accepted 12 November 2024; Published 01 December 2024

Abstract

This study enriches structural optimization research using direct analysis for steel truss structures, which is often hampered by high computational demands. The main objective of this work is to evaluate multi-objective optimization algorithms in truss sizing optimization with discrete variables, focusing on minimizing total mass and controlling inter-story drift under multiple load combinations. Five leading multi-objective metaheuristic algorithms were assessed: SPEA2, GDE3, NSGA2, MOEA/D, and the novel MOEA/D-EpDE, which uniquely combines MOEA/D with Dynamical Resource Allocation and pbest Differential Evolution. Four performance indicators, such as Generational Distance (GD), GD Plus (GD+), Inverted GD+ (IGD+), and Hypervolume (HV), were utilized. Findings from four truss optimization problems revealed that all considered algorithms located feasible optimal solutions, but MOEA/D-EpDE excelled, consistently securing the lowest GD, GD+, IGD+, and anchor point values, along with the highest HV values in most scenarios. This indicates its superior capability in addressing the problem efficiently. NSGA2 and MOEA/D also performed well, outperforming GDE3 and SPEA2. This study is pioneering in its application of these algorithms to steel truss optimization via direct analysis, highlighting the potential for advanced computational techniques in structural engineering.

Keywords: Optimization; Direct Analysis; Truss; Multi-Objective; Metaheuristic; Discrete.

1. Introduction

Direct analysis offers several advantages over conventional methods based on linear analysis, including: (1) accounting for the nonlinear inelastic responses of structures, (2) considering the redistribution of internal forces within the structure, and (3) evaluating the structural load-bearing capacity, thereby simplifying the assessment of structural performance. With direct analysis, the tedious and complex process of individually checking each structural component, as required in member-based analysis methods, becomes unnecessary. With the robust computational power available today, direct analysis methods are increasingly being utilized in structural design, particularly for steel structures, which inherently exhibit nonlinear characteristics. Notable studies that have employed direct analysis for steel truss structures include those referenced in Habibi & Bidmeshki [1] and Thai & Kim [2], among others.

Truss design optimization has been a significant area of research for decades, with hundreds of studies published annually in recent years. This research encompasses various aspects, including problem formulation and the development of optimization algorithms. Truss optimization problems are typically divided into single-objective optimization (SOO) and multi-objective optimization (MOO) categories. Typical objectives in truss optimization include minimizing mass and displacement, with design variables that can be either continuous or discrete. Common

* Corresponding author: thangnn@tlu.edu.vn

http://dx.doi.org/10.28991/CEJ-2024-010-12-07

design constraints involve stress, displacement, bifurcation buckling, and natural frequencies. The presence of nonlinear factors, such as complex search regions, non-convex feasible spaces, nonlinear structural responses, and multiple constraints, can pose challenges for gradient-based optimizers in identifying optimal solutions. Consequently, metaheuristic algorithms (MHs) have become popular alternatives for optimization, appreciated for their enhanced capability to locate global optimal solutions. In particular, Sheng-Xue [3] successfully applied the medalist learning algorithm to address the highly nonlinear optimization challenges of truss structures while considering frequency constraints. Ouardani & Tbatou [4] utilized a genetic algorithm (GA) to develop a two-step optimization procedure for optimizing the layout of seismic isolators. Altay et al. [5] introduced an enhancement to the salp swarm algorithm (SSA) aimed at sizing optimization of planar trusses. Kaveh & Hosseini [6] improved the Bat algorithm by incorporating the Doppler effect to optimize truss structures. Additional noteworthy contributions can be found in references [7-9].

Common advantages of MHs are derivative-free nature, robustness, ease of understanding, and flexibility in coding and implementation. In MOO, another key advantage of MHs is their ability to explore the Pareto front in a single run. MHs are particularly well-suited for truss design involving discrete shape and sizing variables, providing practical solutions by addressing concurrent topology, shape, and sizing problems and accommodating non-differentiable constraints. While MHs offer high-quality solutions, they do not always reach the absolute optimum and require substantial structural analyses to evaluate constraints, leading to excessive computational demands.

Most research on truss optimization has concentrated on SOO, typically focusing on minimizing structural mass while satisfying safety constraints under various combination loads. Over the past three decades, numerous metaheuristic-based optimization algorithms for truss structures have been developed. For example, in 1995, Hajela & Lee [10] utilized a genetic algorithm (GA) to develop a topology optimization procedure of trusses. That same year, Bennage & Dhingra [11] addressed the optimization problem of truss structures using a Tabu search algorithm. In 2008, Lamberti [12] employed a simulated annealing (SA) algorithm to minimize the mass of truss structures while considering numerous constraints. Additionally, Serra & Venini [13] introduced various applications of the ant colony optimization (ACO) algorithm for optimizing planar trusses in 2006. Furthermore, particle swarm optimization (PSO) [14] and differential evolution (DE) [15] were also applied to solve truss optimization problems as early as the 20th century. Over time, numerous algorithms have emerged, including many newly proposed algorithms and improved versions of existing ones. Some interesting algorithms are Jaya [16], the coyote algorithm (COA) [17], and colliding bodies optimization (CBO) [18]. Most studies utilize linear analysis for truss structural analysis, while only a few focus on truss optimization using nonlinear inelastic analysis. Among the limited studies addressing truss optimization with an emphasis on structural nonlinearity, Madah & Amir [19] investigated geometric nonlinearity through co-rotational beam modeling in truss optimization. Missoum et al. [20] developed a displacement-based optimization method specifically for the sizing optimization of nonlinear truss structures. Similarly, Hrinda & Nguyen [21] took geometric nonlinearity into account in the optimization of shallow truss structures. Additionally, Kameshki & Saka [22] optimized the geometry of braced domes by considering geometric nonlinearity. Incorporating direct analysis to account for structural nonlinearity and the discreteness of design variables is anticipated to make truss structure optimization significantly more complex and nonlinear than traditional truss optimization problems. Given the ongoing development of new MHs, it is essential to compare their performance to identify the most effective algorithms for specific optimization problems, potentially revealing powerful new methods.

In the context of MOO for truss structures, there has been significantly less research compared to SOO problems. However, real-world design tasks typically involve multiple objectives to meet various cost and technical requirements. Designers often seek an optimal set of trade-off solutions based on several design criteria to facilitate decision-making. MHs are well-suited for MOO of trusses due to their ability to effectively generate such solutions in a single run while also requiring fewer function evaluations. Based on MHs, many multi-objective MH algorithms (MOMHs) have been developed, including multi-objective evolutionary algorithm based on decomposition (MOEA/D) [23], nondominated sorting genetic algorithm-II (NSGA2) [24], strength Pareto evolutionary algorithm (SPEA) [25], generalized differential evolution 3 (GDE3) [26], among others. Several notable studies have addressed the multi-objective optimization (MOO) of trusses, with most of the published works on linear structures.

For instance, Gholizadeh & Fattahi [27] optimized steel structures under seismic loading using a performance-based design approach. Eid et al. [28] extended the Water Cycle Algorithm (WCA) to a multi-objective framework for optimizing truss structures. Kaveh & Ilchi Ghazaan [29] applied the vibrating particles system (VPS) to tackle MOO problems. Some other interesting topics have also been conducted including natural frequencies and stability [30] and reliability-based MOO [31]. Direct analysis has also been applied in truss MOO problems in very limited quantities. Cao et al. [32] introduced MOEAD-EpDE, a hybrid algorithm combining an improved pbest-based DE with MOEA/D, highlighting its effectiveness in MOO of nonlinear trusses. In a follow-up study, Cao et al. [33] compared six MOMHs for nonlinear inelastic trusses but focused predominantly on continuous design variables. While numerous MOO algorithms and problems exist, there is a critical need for studies evaluating MOMH performance across distinct classes of MOO challenges. Addressing this need, Panagant et al. [34] conducted a comparative study of sixteen MOMHs specifically for truss optimization. Furthermore, Panagant et al. [35] examined MOMH performance in many-objective optimization of truss structures using four objectives: mass, compliance, first natural frequency, and buckling factor. Despite these efforts, existing research largely limits its scope to linear analysis and continuous design variables, leaving a gap in the literature regarding the evaluation of MOMHs under conditions involving discrete variables and nonlinear structural behavior.

To contribute to the literature, we have, for the first time, conducted a comparison of MOMHs for the MOO of truss structures considering discrete variables using direct analysis. The design problem aims to optimize structural mass and inter-story drift or nodal displacements under multiple load combinations, using direct analysis to accurately capture the structure's nonlinear inelastic responses. Five prominent and contemporary multi-objective metaheuristic algorithms (SPEA2, GDE3, NSGA2, MOEA/D, and MOEA/D-EpDE) are evaluated. The study examines four widely used planar and spatial truss structures based on four performance measures. The remainder of the paper is structured as follows: Section 2 details the MOO truss problems using direct analysis. Section 3 briefly describes the MOMHs utilized in this study. The examples considered are examined in Section 4. Finally, Section 5 summarizes the key conclusions and proposes directions for future research.

2. MOO Problem for Trusses using Direct Analysis

2.1. Direct Analysis Model for Steel Trusses

The fundamental principle of direct analysis involves divding the loads applied to the structure into very small load increments, with the structural responses and deformations being systematically recorded at each step. This approach enables direct capture of the nonlinear force-displacement relationship, which is crucial for determining the structure's ultimate load-carrying capacity which can be represented by the ultimate load factor (ULF). The structure is considered safe when the ULF is at least 1.0. Consequently, this method eliminates the need for the detailed safety checks of individual members required in linear analysis.

In this study, we utilize the Practical Advanced Analysis Program (PAAP) [2] to determine ULF of steel trusses. The accuracy and reliability of PAAP have been well-documented in various studies within the literature, as cited in [36-38]. In PAAP, to capture the nonlinear response of an element, the constitutive model developed by Blandford [39] is employed. This model accounts for all key modes, including compression, tension, buckling, post-buckling, and post-yielding. Detailed equations describing these behavior curves are provided in Blandford [39]. The element equation, expressed in an incremental form, is as follows Yang & Kuo [40]:

$$([k_E] + [k_G] + [s_1] + [s_2] + [s_3])\{d\} = \{^2f\} - \{^1f\} \tag{1}$$

Here, ^1f and ^2f are nodal forces at two states; $[k_E]$ and $[k_G]$ denote stiffness matrices of elasticity and geometry; and, $[s_1]$, $[s_2]$, and $[s_3]$ are higher-order stiffness matrices that account for the axial strain's nonlinear component. The Generalized Displacement Control (GDC) technique [41] is applied to handle the above nonlinear equation, effectively computing the equilibrium path with multiple limit points.

2.2. MOO of Steel Trusses with Discrete Design Variables

In an MOO problem, at least two conflicting objectives are evaluated. Typically, structural optimization includes minimizing the total cost or mass to ensure economic efficiency. Here, the structural members' cross-sections aim to minimize total cost/weight while satisfying design requirements for strength, serviceability, and constructability. However, smaller cross-sections can reduce stiffness and safety. To counter this, the maximum inter-story drift is often the second objective, as minimizing these can enhance global stiffness. Other potential objectives in structural design may include failure probability, cross-section types, and natural frequencies, among others. In this work, a bi-objective optimization problem with discrete design variables for steel trusses using direct analysis is to minimize the following objectives:

$$F_1(X) = \rho \sum_{i=1}^{D} \sum_{j=1}^{N_j} A(x_i) L_{ij} \tag{2}$$

$$F_2(X) = \sqrt{\sum_{k=1}^{N_{story}} (d_k)^2} \tag{3}$$

Where ρ is the material weight density, $\mathbf{X} = (x_1, \dots x_D)$ is the vector of design variables where D is the number of design variables, $A(x_i)$ is the cross-sectional area for the design variable i^{th} in which x_i the order of the selected section in the given discrete set of sections, L_{ij} is the length of the truss element j^{th} in the member group i^{th}, N_j is the number of structural elements having the sectional-area $A(x_i)$, d_k is the inter-story drift of story k^{th}, and N_{story} is the number of structural stories. Equation 3 can also be expressed in terms of nodal displacements.

The strength constraints align with the strength load combinations. When using nonlinear inelastic analysis, structural safety is assessed in the view of the ultimate load factor *ULF:*

$$C_l^{strength} = 1 - ULF_l \leq 0 l = 1, .., N_{strength} \tag{4}$$

For serviceability, the inter-story drifts are ensured as:

$$C_j^{service} = \max_{k=1,N_{story}} \left(\frac{|d_{k,j}|}{d_{k,j}^u} \right) - 1 \leq 0 j = 1, .., N_{service} \tag{5}$$

In which $d_{k,j}^u$ is the limit of $d_{k,j}$.

In this study, the penalty function method is utilized for constraint handling due to its simplicity and ease of use, leading to a reformulation of Equations 2 and 3 as:

$$F_1^{un}(X) = F_1(X) \times \left(1 + \sum_{l=1}^{N_{strength}} \alpha_{str,l} \max\left(C_l^{strength}, 0\right) + \sum_{j=1}^{N_{service}} \alpha_{disp,j} \max\left(C_j^{service}, 0\right)\right) \tag{6}$$

$$F_2^{un}(X) = \left(1 + \sum_{l=1}^{N_{strengt\square}} \alpha_{str,l} \max\left(C_l^{strengt\square}, 0\right) + \sum_{j=1}^{N_{service}} \alpha_{disp,j} \max\left(C_j^{service}, 0\right)\right) \times F_2(X) \tag{7}$$

where $\alpha_{str,l}$ and $\alpha_{disp,j}$ are the penalty parameters to eliminate infeasible candidates during the optimization process by assigning large values

3. Optimization Algorithms

To address MOO problems, three main methods have been developed: (1) converting the problem into a SOO by combining individual objectives using a weighted sum method, (2) converting it into SOO by retaining one objective and transforming others into constraints, and (3) finding the Pareto front directly. The first method involves creating various SOO problems by adjusting weighting coefficients, suitable for solving with MHs. However, it requires significant computational effort, struggles with nonconvex spaces, and can be inefficient due to arbitrary coefficient selection. The second method transforms MOO into SOO by varying constraint values, but arbitrarily selecting these values poses challenges similar to the first method, though it handles nonconvex spaces better. The third method uses MOMHs tailored for MOO to find the entire Pareto front effectively, as these algorithms handle a population of solutions and are adept at locating global optima in complex, nonlinear, and non-convex problems. Accordingly, this study concentrates on MOMHs, specifically NSGA2, GDE3, SPEA2, MOEA/D, and MOEAD-EpDE with following detailed descriptions.

3.1. NSGA2

NSGA2 [42, 43] is a pioneering multi-objective optimization (MOO) method. NSGA2 follows the basic framework of a genetic algorithm (GA), which draws inspiration from Darwin's evolutionary theory. In a typical GA, the next generation's individuals, or chromosomes, are derived from "good" parents (individuals/chromosomes from the current generation) using mutation, crossover, and selection. Traditionally, a chromosome is represented in binary form with genes set as 1 or 0. Offspring are created by selecting two parent chromosomes using methods like roulette wheel, event selection, or rank-grounded selection to identify superior parents. These parents undergo crossover (such as one-point or two-point crossover) where genetic material is exchanged. A mutation operator with small rate changes gene values in the offspring to avoid local optima. An "elitist selection" keeps the best individual for quality assurance in the next generation. NSGA2 improves the process for MOO by integrating fast nondominated sorting and crowded comparison sorting. Fast nondominated sorting classifies individuals into nondomination fronts using domination count nt, representing how many solutions dominate a solution p, and the set Sp of solutions that p dominates, optimizing computational costs for sorting. Crowded comparison, using nondomination rank and crowding distance, ensures a diverse population by favoring solutions on lower ranks or in less crowded areas. NSGA2 employs simulated binary (SBX) for crossover and polynomial mutation operators, detailed in Zitzler & Thiele [44] and Zitzler et al. [45]. The main procedure of NSGA2 is presented in Figure 1.

3.2. GDE3

GDE3 [26] is an advanced variant of the DE algorithm designed for solving MOO problems. Originating from the robust framework of DE, GDE3 extends the capabilities of its predecessors by efficiently handling multiple conflicting objectives with improved adaptability and diversity management. The algorithm operates by maintaining a population of candidate solutions, characterized by vectors representing potential solutions in the search space. Each solution undergoes mutation, crossover, and selection processes to explore and exploit the search space effectively.

In GDE3, the mutation strategy DE/rand/1/bin from DE is employed to create trial vectors. This mutation operator creates trial vectors by perturbing a target vector using a weighted difference between two randomly selected population vectors, thereby enhancing exploration and helping the algorithm avoid local optima. The crossover process, equally crucial, merges trial vectors with current ones to produce offspring, fostering variability and promoting genetic diversity. The success of these offspring in populating the next generation relies on selection mechanisms tailored for multi-objective contexts. Following the selection operation in GDE3, the population size can initially increase from NP to 2NP after a generation. However, it is then reduced back to NP by applying fast nondominated sorting and crowding distance techniques from NSGA2. These methods ensure that solutions not only converge to the Pareto front but also maintain a well-distributed presence across it. Figure 2 presents the flowchart of GDE3.

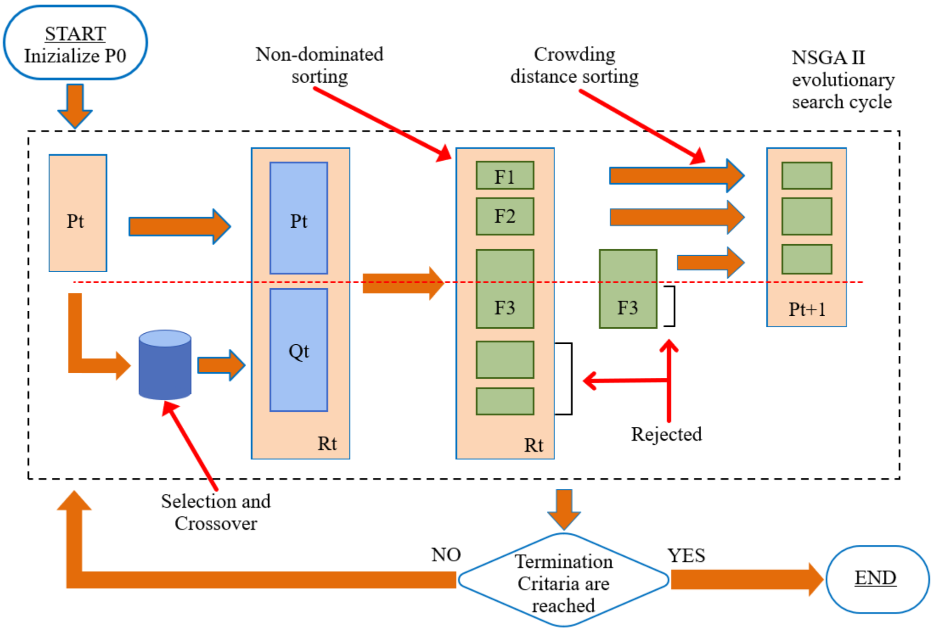

Figure 1. The flowchart of NSGA2

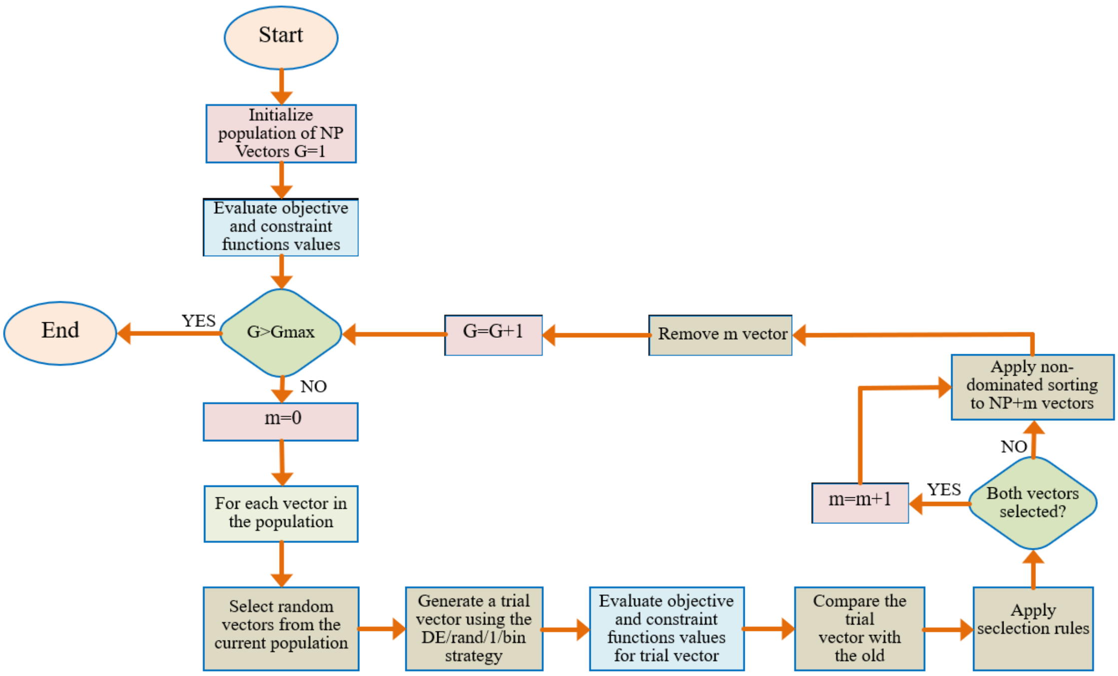

Figure 2. The flowchart of GDE3

3.3. SPEA2

SPEA2 [46] significantly enhances the performance of its predecessor. It incorporates a fitness assignment strategy based on the strength of dominance, where each individual is assigned a fitness score according to how many other solutions it dominates and its proximity to other solutions in the objective space. SPEA2 stores non-dominated solutions in an external archive, ensuring diversity and preventing the loss of optimal solutions over generations. Additionally, it introduces a refined clustering technique to improve diversity within the population, allowing it to maintain a better spread of solutions across the Pareto front. The flowchart of SPEA2 is presented in Figure 3.

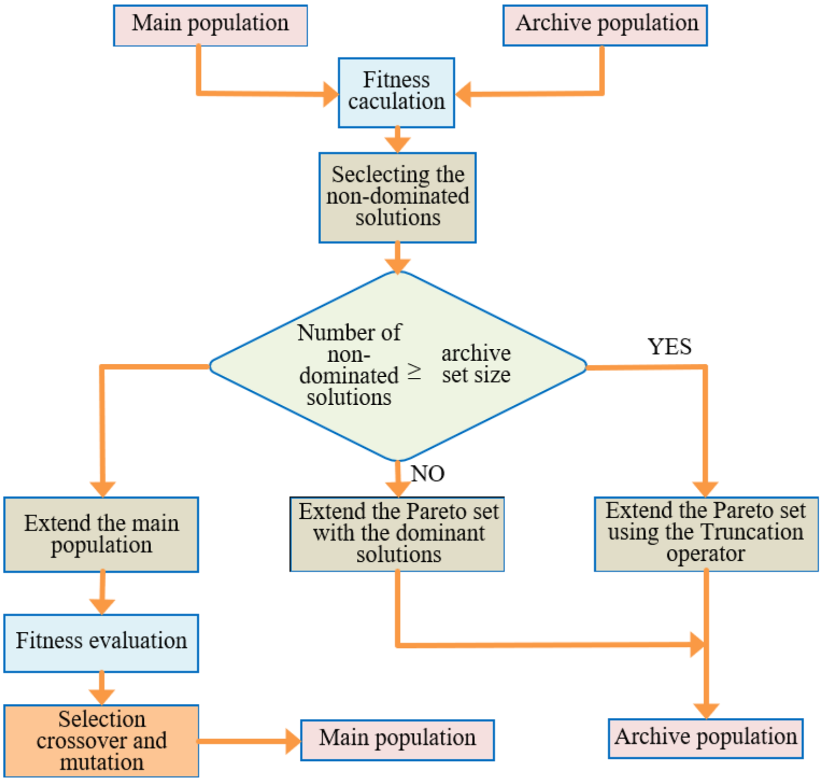

Figure 3. The flowchart of SPEA2

3.4. MOEA/D

MOEA/D, an evolutionary algorithm-based framework, innovatively decomposes an MOO problem into multiple SOO sub-problems [46]. These sub-problems are solved simultaneously and cooperatively, utilizing several evolutionary operators. The approach involves leveraging solutions from neighboring sub-problems to achieve and combine optimal solutions, aiming for Pareto points as illustrated in Figure 4. The primary solution of each sub-problem is derived from its neighbors, facilitating efficient exploration of the solution space.

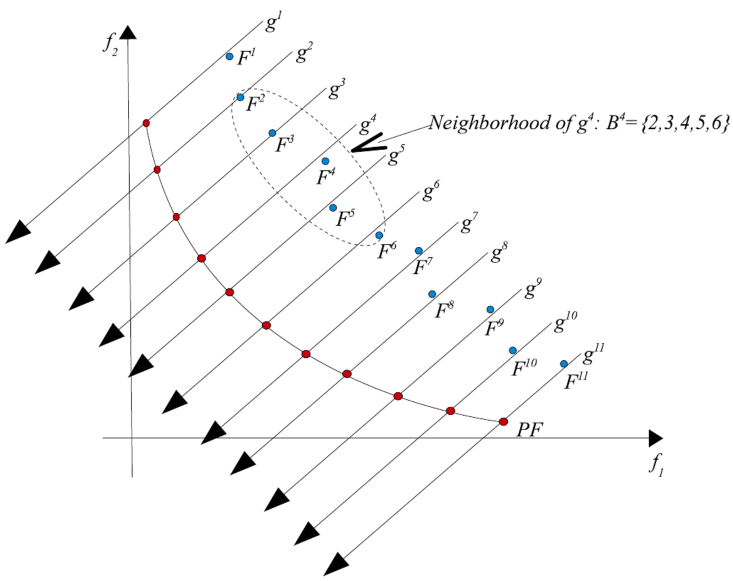

Figure 4. Neighborhood idea in MOEA/D

The weighted Tchebycheff method, renowned for its decomposition capabilities, is suitable for breaking down MOO problems, especially those with non-convex Pareto fronts. However, it typically performs best with MOO problems that have normalized objective functions. The procedure of MOEAD is presented in Figure 5.

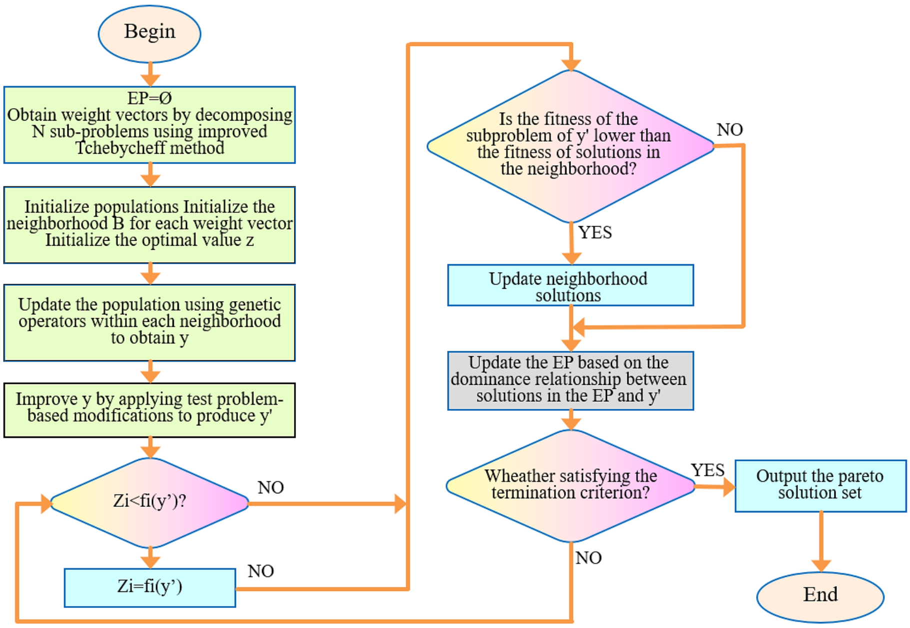

Figure 5. The procedure of MOEA/D

3.5. MOEAD-EpDE

MOEA/D-EpDE [33] represents one of the newest MOO algorithm advancements. It uniquely integrates the strengths of two distinct approaches: the recently developed pbest Differential Evolution (EpDE) algorithm and the MOEA/D with Dynamic Resource Allocation (MOEA/D_DRA). In MOEA/D-EpDE, the framework of MOEA/D_DRA is central to the optimization process. By employing DRA techniques, MOEA/D_DRA is able to manage computational resources efficiently across different sub-problems. This dynamic allocation ensures that computational efforts are focused where they are most needed, enhancing the overall problem-solving efficiency.

Each sub-problem within this framework is tackled using EpDE operators, which are known for their efficiency and effectiveness in finding optimal solutions. Additionally, MOEA/D-EpDE incorporates an external archive to store more non-dominated solutions discovered during the optimization process. This archive plays a crucial role in boosting the algorithm's performance by preserving a diverse set of high-quality solutions. By retaining these non-dominant solutions, the archive helps in improving the diversity of solutions over consecutive iterations, thereby enhancing the exploration capabilities of the algorithm. The entire procedure of the MOEA/D-EpDE, including its structure and workflow, is visually represented and summarized in Figure 6.

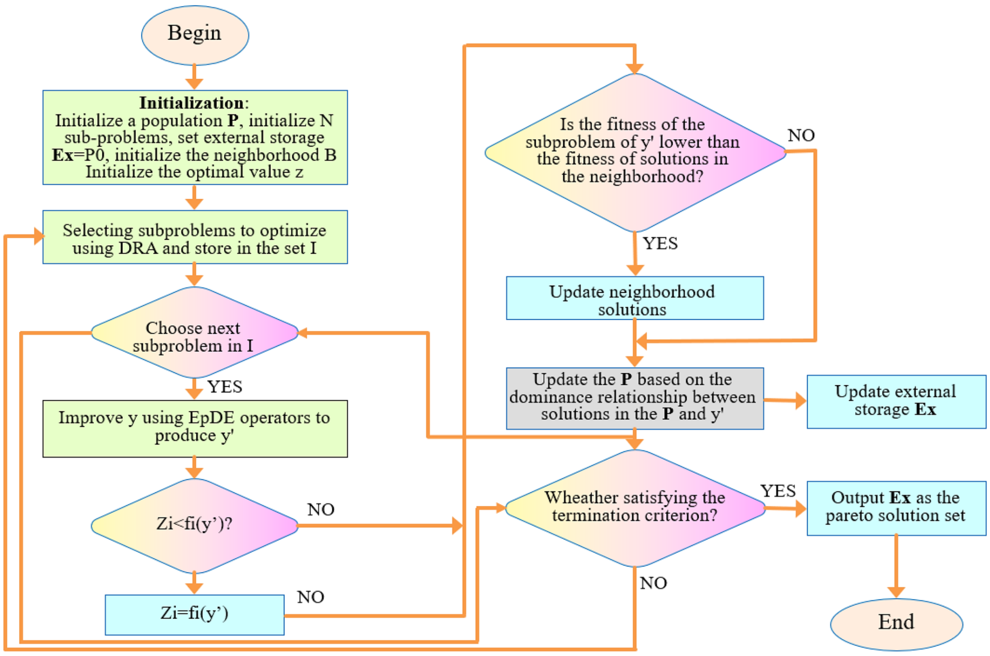

Figure 6. The procedure of MOEAD-EpDE

4. Numerical Examples

4.1. Truss Design Problems

In this section, we evaluate four truss structures with the layout and geometry presented in Figure 7. Comprehensive details of these case studies are outlined in Table 1. The algorithms used in this analysis were developed in Python, with system parameters optimized through a trial-and-error method to identify appropriate values, as detailed in Table 2. For all scenarios, a population size of 100 was utilized. The first truss analysis runs for 200 iterations, while the remaining studies were conducted over 300 iterations. Each algorithm was executed independently 20 times to mitigate the variability inherent in metaheuristic methods. The analyses were conducted on a computer equipped with an Intel Core i7-8700 processor, operating at a clock speed of 3.20 GHz. The average computational time for each optimization run is provided in Table 1. Clearly, direct analysis is computationally intensive.

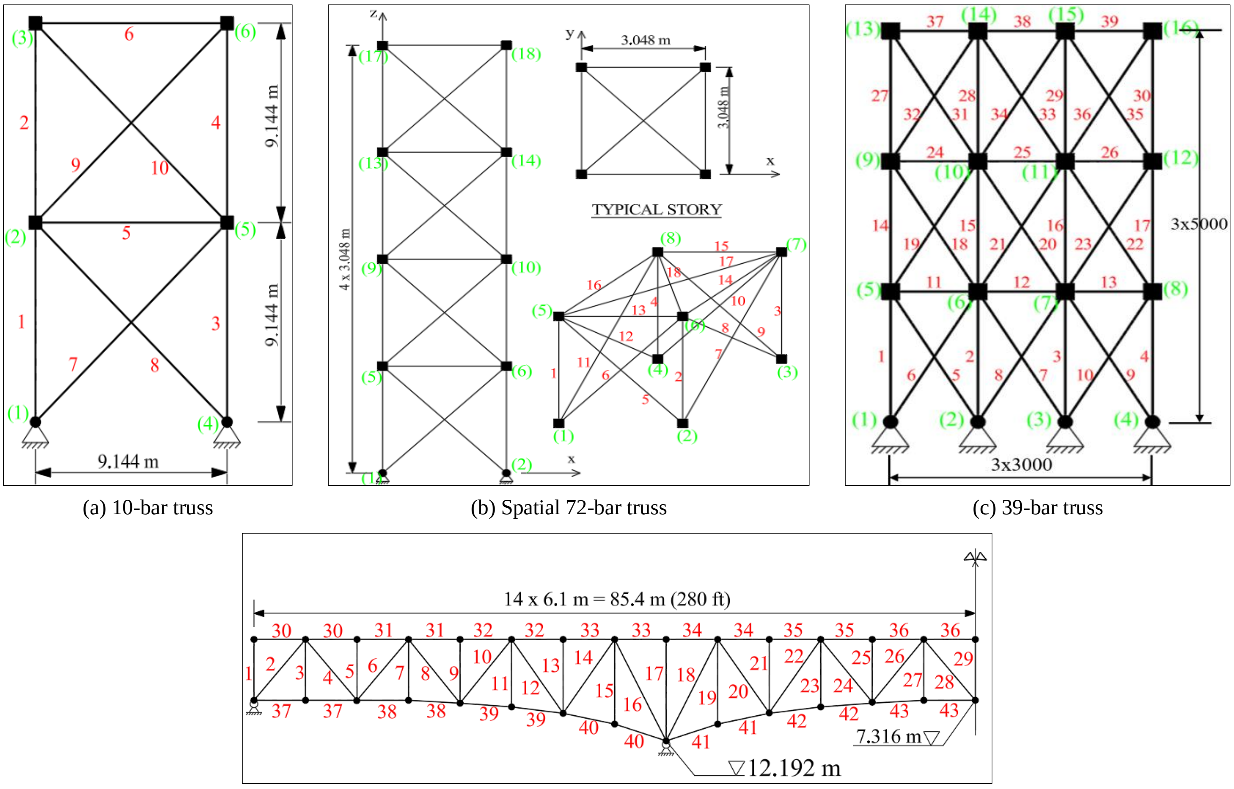

(a) 10-bar truss (b) Spatial 72-bar truss (c) 39-bar truss

(d) 113-bar planar bridge

Figure 7. Truss layouts and geometries

Table 1. Case study information

	Planar 10-bar	Spatial 72-bar	Planar 39-bar	Planar 113-bar bridge
Number of variables	10	16	39	43
Radius of cross-section list (mm)	List [31] = [10-20, 22, 24, 26, 28, 30, 32, 34, 36, 38, 40, 43, 46, 49, 52, 55, 58, 61, 64, 67, 70]	List [31] = [10-20, 22, 24, 26, 28, 30, 32, 34, 36, 38, 40, 43, 46, 49, 52, 55, 58, 61, 64, 67, 70]	List [31] = [10-20, 22, 24, 26, 28, 30, 32, 34, 36, 38, 40, 43, 46, 49, 52, 55, 58, 61, 64, 67, 70]	List [29] = [30-40, 42, 44, 46, 48, 50, 52, 54, 56, 58, 60, 63, 66, 69, 72, 75, 78, 81, 84]
Material	Mass density = 7850 (kg/m^3), yield strength = 344.5 (MPa), Elastic modulus = 200 (GPa)			
Applied loads	DL = 150 (kN), LL = 100 (kN), and W = 100 (kN) at all nodes	DL = 100 (kN), LL = 50 (kN), and W = 40 (kN) at all nodes	DL = 100 (kN), LL = 100 (kN), and W = 60 (kN) at all nodes	DL = 100 (kN) and LL = 50 (kN) at all nodes on upper chord
Load combination	Strength: (1.2DL+1.6LL) and (1.2DL+0.5LL+1.6W) Serviceability: (1.0DL+0.5LL+0.7W)			Strength: (1.25DL+1.75LL), Serviceability: (1.0DL+1.0LL)
Constraints	Strength: ULF $\geq$ 1.0 Serviceability: ULF = 1.0 and interstory drift $\leq$ h/400			Strength: ULF $\geq$ 1.0 Serviceability: ULF = 1.0 and nodal displacement $\leq$ 43.1 (mm)
Objectives	F1 = total mass F2 = $\sqrt{x_1^2 + x_3^2}$	F1 = total mass F2 = $\sqrt{x_5^2 + x_9^2 + x_{13}^2 + x_{17}^2}$	F1 = total mass F2 = $\sqrt{x_5^2 + x_9^2 + x_{13}^2}$	F1 = total mass $F2 = \sqrt{y_1^2 + y_2^2}$ with y_1 and $y_2$of two spans's mid-points
Ave. time computing (second)	6,300	55,800	80,100	228,000

Table 2. Parameters for MOO algorithms

Algorithm	Parameter value
NSGA2	offspring_population_size = population_size; crossover=SBX; mutation = Polynomial; tournament selection
GDE3	DE/rand/1; CR = 0.9; F = 0.1
SPEA2	offspring_population_size = population_size; crossover=SBX; mutation = Polynomial
MOEA/D	CR=1.0; F=0.5; DE/current/1 mutation = Polynomial; neighbor_size=20;
MOEA/D-EpDE	crossover=EpDE_Crossover; External_archive = Enable; mutation = Polynomial; neighbor_size=25;

Four metrics were utilized: GD, GD+, IGD+, and HV. GD calculates the overall distance from computed solutions to the theoretical Pareto front. This measure is further enhanced by GD+, which provides a more refined distance calculation. In contrast, IGD+ focuses on the shortest distance from any given point on the Pareto front to the closest solution within the analyzed set. The HV metric assesses the volume of the objective space that is dominated by the solutions in relation to a predetermined reference point. For these criteria, a more effective algorithm is characterized by achieving lower values in GD, GD+, and IGD+, alongside higher HV results. HV is calculated using a reference point with max objective values plus 1.1. The mathematical formulations for these indicators are detailed in Panagant et al. [34].

4.2. Results of Planar 10-Bar Truss

In structural MOO problems, the true Pareto front is typically unknown, posing a challenge for evaluating the performance of optimization algorithms. To address this, it's a common practice to consider the approximate front constructed by aggregating all optimal solutions found. This aggregated set of solutions provides a comprehensive depiction of the potential Pareto front for the problem at hand. Accordingly, the approximate Pareto front derived from this particular case study is illustrated in Figure 8. This figure not only illustrates the approximate Pareto front but also presents all optimal solutions obtained during the experimental runs, providing a comprehensive visual representation of the solution space explored by the algorithms. The figure reveals variations in the quality of the optimal curves derived from the different runs, with several optimal points situated far from the expected Pareto curve, indicating the varying performance of the MOMHs. This visualization enhances the understanding of solution diversity and distribution, underscoring the optimization method's effectiveness in capturing trade-offs among conflicting objectives. Importantly, all identified optimal solutions comply with the specified constraints, reinforcing initial conclusions regarding the efficiency of the MOO algorithms in identifying optimal solutions for this example. This finding demonstrates the robustness and reliability of the algorithms in generating high-quality outcomes.

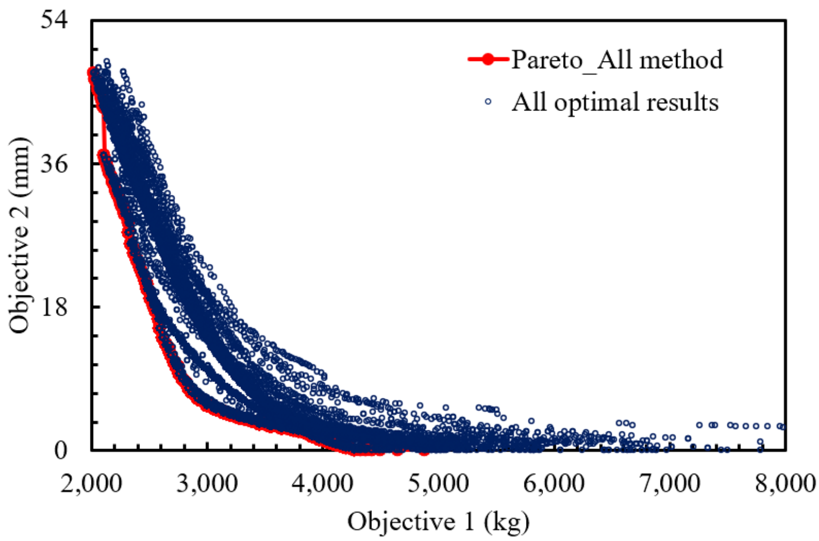

Figure 8. Pareto-front of 10-bar truss

Four indicators (GD, GD+, IGD+, and HV) as well as two anchor points corresponding to the smallest values of each objective were evaluated. Table 3 provides a summary of average GD, GD+, IGD+, HV values, and minimum objective values. Figure 9 presents detailed results for the indicators, while Figure 10 highlights the smallest values for each objective.

Table 3. Performance of MOO algorithms for 10-bar truss

Results	NSGA2	GDE3	SPEA2	MOEA/D	MOEA/D-EpDE
Ave. GD	47.451	89.336	39.343	18.082	16.807
Ave. GD+	47.444	89.334	39.332	18.064	16.781
Ave. IGD+	11.901	18.515	16.475	7.632	9.767
Ave. HV	323,486.0	314,795.7	320,665.6	326,858.2	328,073.9
Best Anchor 1 (Corresponding value of objective function 2)	2,053.1 (46.236)	2,019.1 (47.394)	2,038.6 (46.406)	2,027.9 (47.465)	2,019.1 (4,739.4)
Best Anchor 2 (Corresponding value of objective function 1)	0.013 (5,051.1)	0.009 (4,875.3)	0.053 (4,940.1)	0.010 (6,243.3)	0.015 (5,876.3)

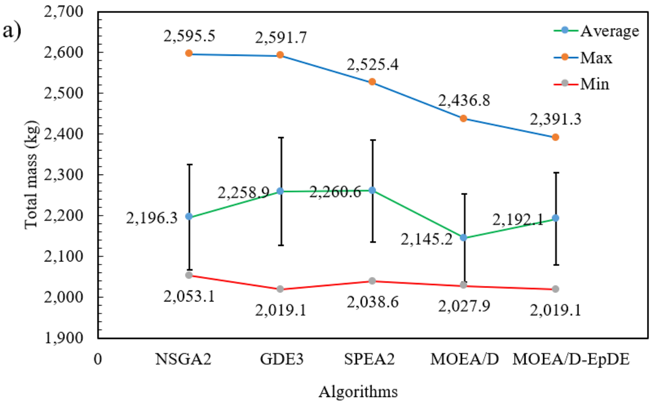

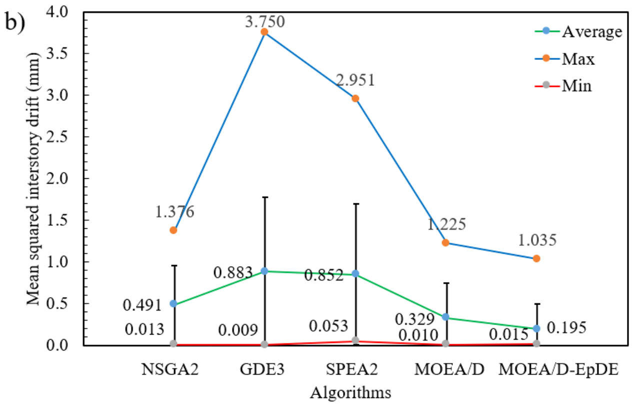

Figure 9. Anchor points for 10-bar truss: a) First objective and b) Second objective

The average GD (Ave. GD) indicates the closeness of the solutions to the Pareto front, with MOEA/D-EpDE achieving the best average GD of 16.807, followed closely by MOEA/D at 18.082, while NSGA2 and GDE3 exhibited significantly larger distances. Similarly, the Ave. GD+ metrics reflect analogous trends. The Ave. IGD+ results further emphasize the superiority of MOEA/D, yielding the lowest average value of 7.632, thereby demonstrating its effectiveness in maintaining solution diversity. The Ave. HV metric, which measures the volume covered by the Pareto front in objective space, also highlights MOEA/D-EpDE as the top performer, with the highest value of 328,073.9. Both best Anchor metrics, which represent performance benchmarks, indicate competitive results among the algorithms, with GDE3 consistently demonstrating robust outcomes. Overall, the data suggest that MOEA/D-EpDE exhibit strong performance across multiple criteria, validating their efficacy as optimization methods in this context.

The relationship between the two objective functions is elucidated in Figure 8 and Table 3. As illustrated in Figure 8, the two objectives are inherently conflicting: reducing the value of objective function 1, which represents the total mass of the structure, necessitates an increase in the value of objective function 2, the squared value of nodal displacements. This inverse relationship is further corroborated by the anchor results presented in Table 3. Specifically, anchor point 1, which corresponds to the minimum value of objective function 1, exhibits a significantly large value for objective function 2. Conversely, anchor point 2, associated with the minimum value of objective function 2, results in a substantially large value for objective function 1. These findings highlight the trade-offs involved in selecting a design solution. Opting solely to minimize the structure's mass (objective function 1) leads to larger nodal displacements, thereby decreasing structural stiffness. In contrast, minimizing nodal displacements results in a heavier structure. This analysis underscores the importance of balancing these objectives to achieve an optimal design that meets both performance and efficiency criteria.

Figures 9-a to 9-d illustrate MOEA/D-EpDE's top performance in all four indicators. Specifically, it recorded the smallest GD (the minimum and maximum values of 0.147 and 52.522, respectively), the smallest GD+ (the minimum and maximum values of 0.096 to 52.522, respectively), the lowest maximum IGD+ (27.943), the second-lowest minimum IGD+ (1.658), and the highest HV (336,772). Figs. 10a-b further affirm MOEA/D-EpDE’s efficiency with the lowest maximum anchor values (2,391.3 kg and 1.035 mm). Thus, MOEA/D-EpDE is conclusively the best algorithm in this study, followed by MOEA/D, NSGA2, GDE3, and SPEA2, respectively.

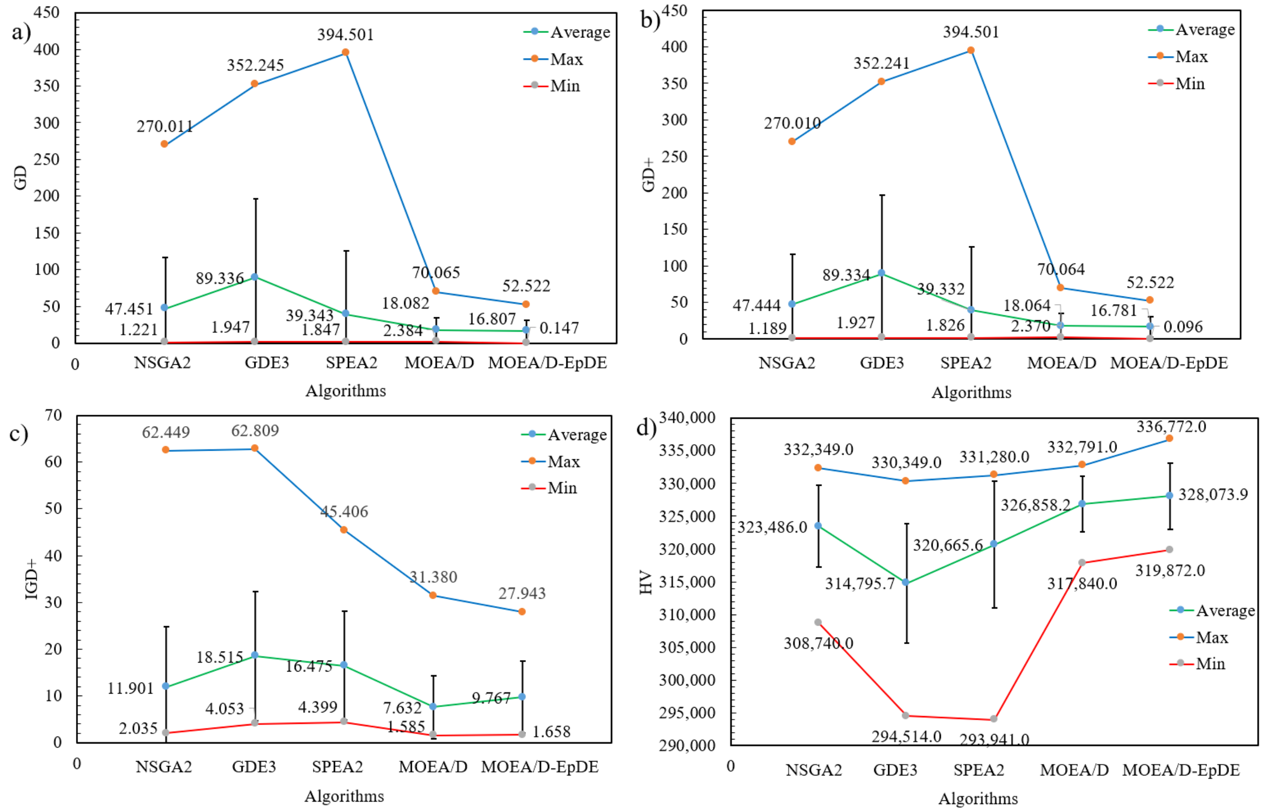

Figure 10. Performance indicators for 10-bar truss: a) GD, b) GD+, c) IGD+, and d) HV

4.3. Results of Spatial 72-Bar Truss

Figure 11 illustrates the approximate Pareto front derived from this case study. Notably, all identified optimal solutions satisfy the established constraints, reinforcing initial conclusions regarding the effectiveness of the MOO algorithms used in this example. This outcome underscores the robustness and reliability of the algorithms in generating high-quality results within the constraints of the problem.

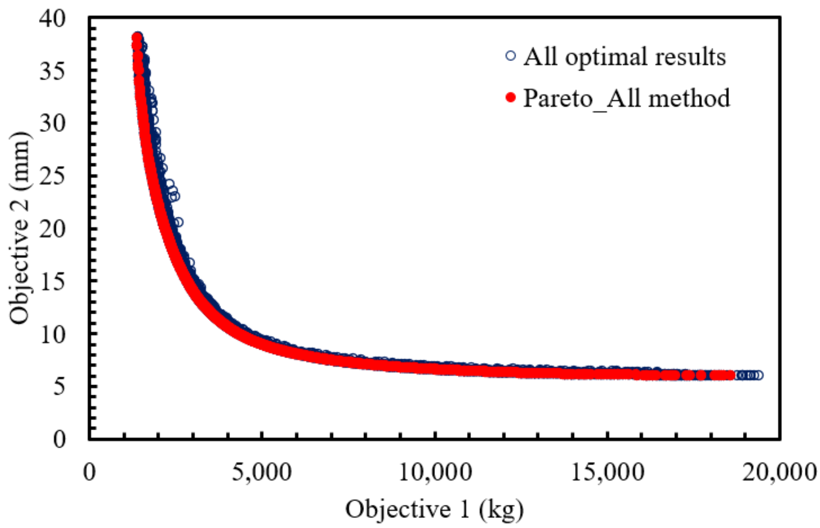

Figure 11. Approximate Pareto-front for 72-bar truss

Table 4 summarizes the performance metrics of the five optimization algorithms, including average GD, GD+, IGD+, HV values, and minimum objective values. Complementary results for these indicators are illustrated in Figure 12, while Figure 13 highlights the smallest values attained for each objective. The data indicate that MOEA/D-EpDE exhibits superior overall performance, achieving the lowest average values for GD (0.509), GD+ (0.114), and IGD+ (0.325). These results suggest a closer approximation to the Pareto front and high-quality solutions. Additionally, MOEA/D-EpDE secures the highest average HV (670,619.5), which signifies the largest dominated objective space among the algorithms. Concerning anchor points, MOEA/D-EpDE also reports the lowest values for Best Anchor 1 (1,364.800) and Best Anchor 2 (6.085), indicating its capability in identifying optimal solutions. MOEA/D performs admirably, closely trailing MOEA/D-EpDE, especially in terms of GD. This is corroborated by the findings presented in Figures 12 and 13, which reveal that the distribution of GD, GD+, IGD+, and HV indicators for MOEA/D-EpDE is notably superior to those of other algorithms. In the rankings, NSGA2 and MOEA/D secure the second and third positions, respectively, with NSGA2 outperforming in GD, GD+, HV, and Best Anchor 1, while MOEA/D excels in IGD+ and Best Anchor 2. GDE3 and SPEA2 are identified as the least effective algorithms in this context.

Table 4. Performance of MOO algorithms for spatial 72-bar truss

Results	NSGA2	GDE3	SPEA2	MOEA/D	MOEA/D-EpDE
Ave. GD	0.545	0.982	0.629	0.510	0.509
Ave. GD+	0.204	0.731	0.263	0.113	0.114
Ave. IGD+	0.447	1.193	7.715	1.126	0.325
Ave. HV	669,340.3	666,425.4	661,324.0	668,437.8	670,619.5
Best Anchor 1 (Corresponding value of objective function 2)	1,374.5 (37.412)	1,422.5 (36.015)	1,623.6 (34.833)	1,430.6 (37.823)	1,364.8 (38.109)
Best Anchor 2 (Corresponding value of objective function 1)	6.139 (15,620.8)	6.092 (17,963.9)	6.135 (15,536.8)	6.091 (18,207.8)	6.085 (18,577.6)

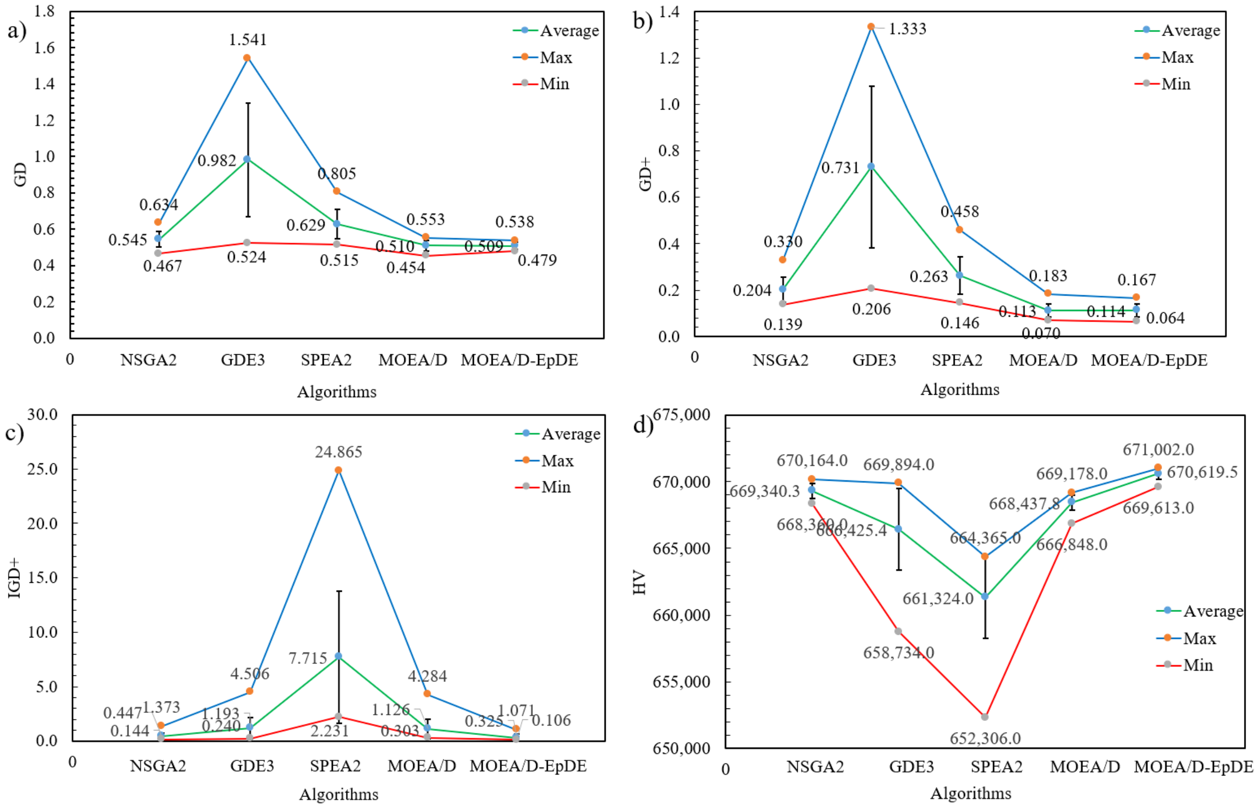

Figure 12. Performance indicators for 72-bar truss: a) GD, b) GD+, c) IGD+, and d) HV

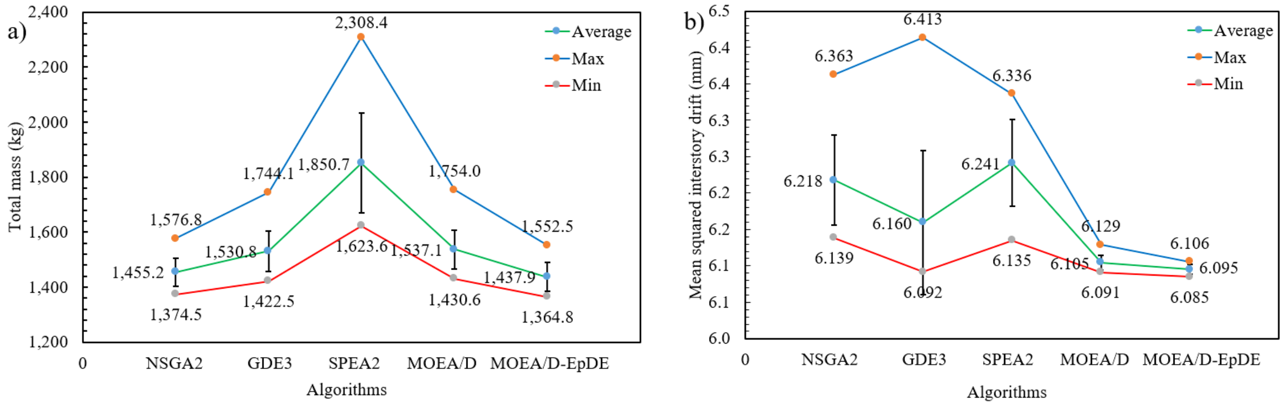

Figure 13. Anchor points for 72-bar truss: a) First objective and b) Second objective

Similar to the first example, the two objective functions are illustrated in Figure 11 and Table 4. The data reveal a fundamental conflict: reducing the total mass of the structure (objective function 1) leads to increased squared nodal displacements (objective function 2). Specifically, anchor point 1, representing the minimum mass, corresponds to a high value for objective function 2, while anchor point 2, indicating minimized nodal displacements, results in a significant mass increase. These findings emphasize the trade-offs in design choices, highlighting the need to balance mass reduction with nodal displacement to achieve an optimal, efficient structure.

4.4. Results of Planar 39-Bar Truss

Figure 14 illustrates the approximate Pareto front obtained from the analyzed structure, demonstrating that all identified optimal solutions comply with the established constraints. This outcome underscores the effectiveness of the optimization algorithms utilized in this study, as they not only generate high-quality solutions but also ensure adherence to the specified requirements. The ability of these algorithms to consistently meet the constraints while achieving optimal solutions further highlights their robustness and reliability in addressing complex optimization problems.

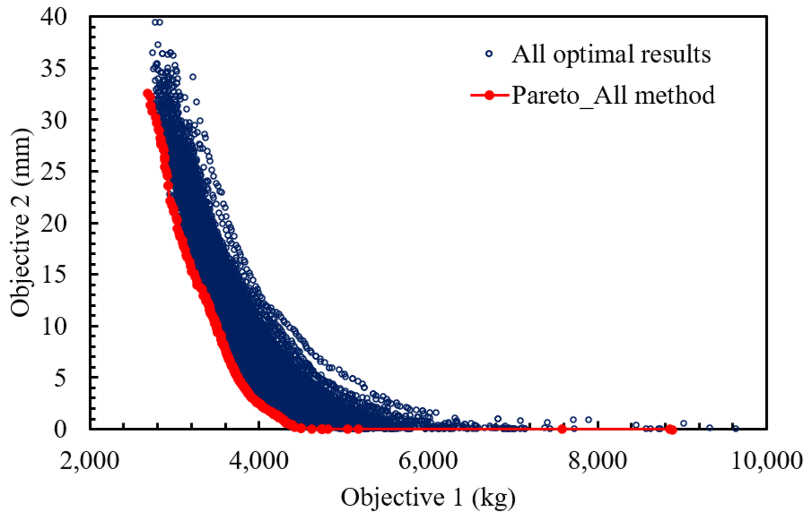

Figure 14. Approximate Pareto-front for 39-bar truss

Table 5 summarizes the performance metrics of the optimization algorithms, including average GD, GD+, IGD+, HV values, and minimum objective values. Figure 15 provides a detailed representation of these indicators, while Figure 16 highlights the smallest values achieved for each objective. The data reveals that MOEA/D-EpDE excels with the lowest average GD (2.497) and GD+ (2.479), indicating its superior proximity to the Pareto front. Furthermore, it achieves the lowest average IGD+ (6.142) and the highest HV (392,809.3), reflecting a more extensive exploration of the objective space. MOEA/D-EpDE's exceptional performance is also evident in its Best Anchor 1 (2,740.300) and Best Anchor 2 (0.003) values, showcasing its capability to consistently identify optimal solutions. While NSGA2 and SPEA2 deliver competitive results in GD and GD+ metrics, they fall short in IGD+ and HV comparisons. Overall, MOEA/D-EpDE demonstrates remarkable effectiveness across the evaluated algorithms, a conclusion supported by the data presented in Figures 15 and 16. Notably, the distribution across the GD, GD+, IGD+, and HV indicators for MOEA/D-EpDE is superior to those of the other algorithms. NSGA2 and GDE3 follow in the second and third positions, respectively. In this analysis, SPEA2 and MOEA/D rank as the least effective algorithms, underscoring the robustness of the alternatives. Additionally, as seen in Figure 14 and Table 5, the two objective functions exhibit a fundamental conflict: minimizing the total mass of the structure (objective function 1) results in increased squared nodal displacements (objective function 2). Anchor point 1, which represents minimal mass, correlates with a high value for objective function 2, while anchor point 2, which minimizes nodal displacements, leads to a significant increase in mass. These findings underscore the trade-offs in design choices, necessitating a balance between mass reduction and nodal displacement for optimal efficiency.

Table 5. Performance of MOO algorithms for planar 39-bar truss

Results	NSGA2	GDE3	SPEA2	MOEA/D	MOEA/D-EpDE
Ave. GD	4.780	5.461	4.027	7.938	2.497
Ave. GD+	4.774	5.452	4.018	7.934	2.479
Ave. IGD+	6.811	16.158	16.084	6.537	6.142
Ave. HV	385,929.4	382,729.6	383,587.2	384,001.6	392,809.3
Best Anchor 1 (Corresponding value of objective function 2)	2,780.9 (32.389)	2,841.9 (32.428)	2,754.0 (31.496)	2,753.6 (34.901)	2,740.3 (32.965)
Best Anchor 2 (Corresponding value of objective function 1)	0.025 (6,466.2)	0.018 (6,952.0)	0.031 (5,586.4)	0.028 (11,276.8)	0.003 (8,874.4)

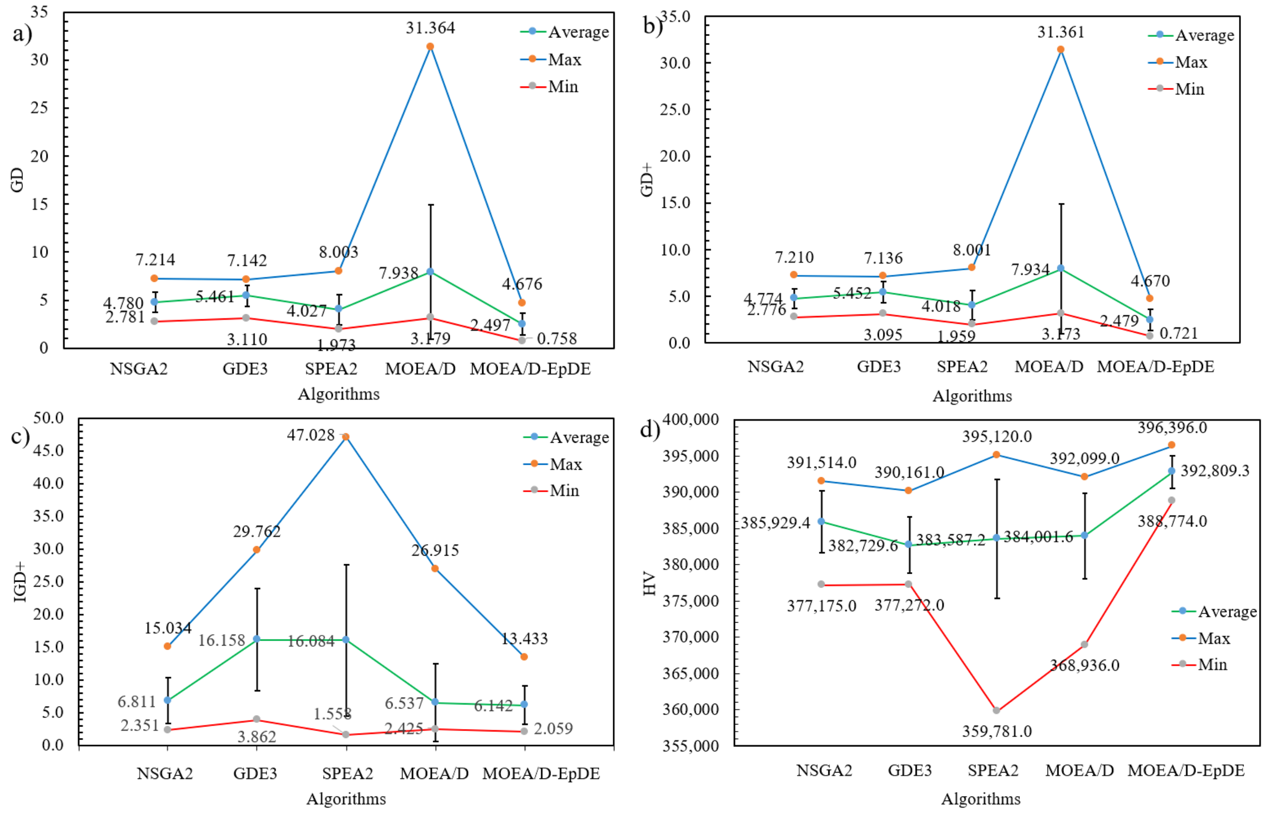

Figure 15. Performance indicators for 39-bar truss: a) GD, b) GD+, c) IGD+, and d) HV

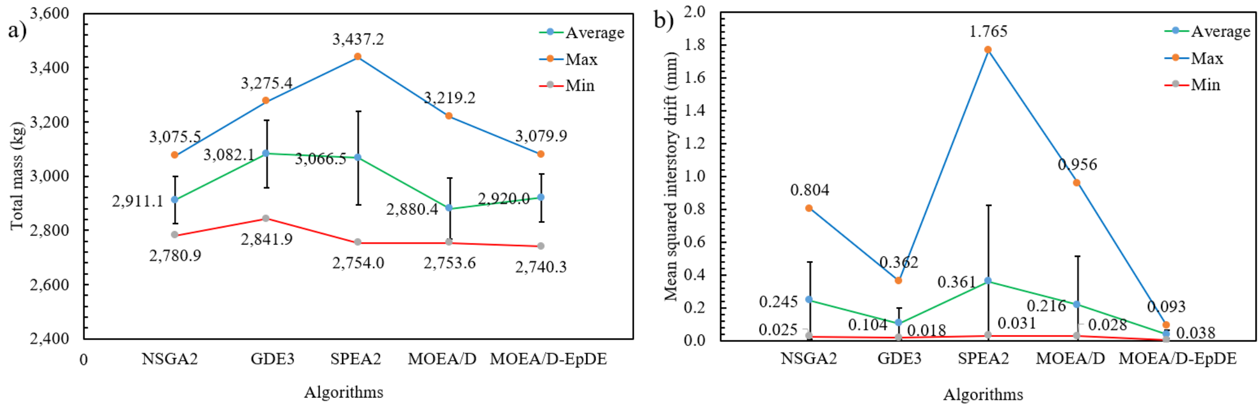

Figure 16. Anchor points for 39-bar truss: a) First objective and b) Second objective

4.5. Results of 113-Bar Plane Truss Bridge

Figure 17 depicts the approximate Pareto front constructed from all optimal solutions derived across all algorithms runs. The figure confirms that each identified solution complies with the established constraints, demonstrating the robustness and reliability of these algorithms in addressing this MOO problem.

Table 6 summarizes the performance metrics of various optimization algorithms, presenting average values for GD, GD+, IGD+, HV, and minimum objective values. For a more granular analysis, Figure 18 displays detailed results for these performance indicators, while Figure 19 highlights the smallest values achieved for each objective. Consistent with previous findings, MOEA/D-EpDE emerges as the leading algorithm, achieving the lowest average GD of 2.614 and GD+ of 0.171, indicating its superior closeness to the Pareto front. Additionally, MOEA/D-EpDE registers an impressive average IGD+ of 7.799 and the highest HV value of 3,886,832.0, signifying a comprehensive exploration of the objective space. In terms of anchor point performance, MOEA/D-EpDE also demonstrates competitiveness with values of 48,824.0 for Best Anchor 1 and 29.682 for Best Anchor 2. While MOEA/D also performs commendably with a solid average IGD+, other algorithms such as NSGA2, GDE3, and SPEA2 lag behind in these metrics, particularly in terms of HV and IGD+. Overall, the results affirm that MOEA/D-EpDE demonstrates the most effective performance across all evaluated criteria. This conclusion is further corroborated by the data illustrated in Figures 18 and 19, which distinctly show MOEA/D-EpDE's excellence in GD, GD+, IGD+, and HV metrics relative to its counterparts. Following MOEA/D-EpDE, the algorithms MOEA/D, NSGA2, and SPEA2 rank in the subsequent positions, showcasing relatively strong performance. However, GDE3 ranks the lowest among the evaluated algorithms in this study, indicating its lesser effectiveness across the assessed indicators. This highlights the variability in performance outcomes among the algorithms and emphasizes the advantages of MOEA/D-EpDE in multi-objective optimization contexts. Furthermore, Figure 17 and Table 6 reveal a fundamental conflict between the objective functions: minimizing structure mass (objective function 1) increases squared nodal displacements (objective function 2). This highlights the trade-offs in design decisions, emphasizing the need to balance mass reduction with nodal displacement for optimal efficiency.

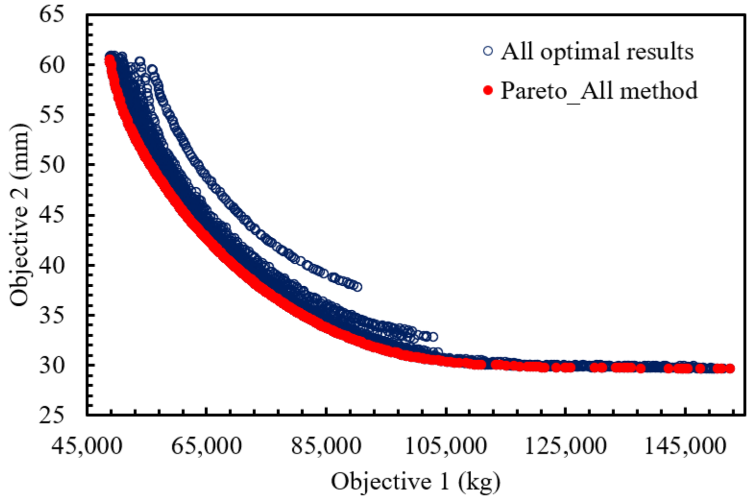

Figure 17. Approximate Pareto-front for 113-bar truss bridge

Table 6. Performance of MOO algorithms for 113-bar plane truss bridge

Results	NSGA2	GDE3	SPEA2	MOEA/D	MOEA/D-EpDE
Ave. GD	2.719	3.546	2.806	2.681	2.614
Ave. GD+	0.536	1.933	0.523	0.428	0.171
Ave. IGD+	39.764	73.474	94.668	41.750	7.799
Ave. HV	3,499,574.7	3,640,618.7	3,504,528.0	3,841,450.7	3,886,832.0
Best Anchor 1 (Corresponding value of objective function 2)	48,809.0 (60.429)	49,592.0 (59.923)	50,656.0 (58.931)	49,795.0 (60.563)	48,824.0 (40.461)
Best Anchor 2 (Corresponding value of objective function 1)	32.762 (90,365.2)	30.335 (107,342.7)	32.915 (91,126.0)	29.686 (145,864.4)	29.682 (147,634.6)

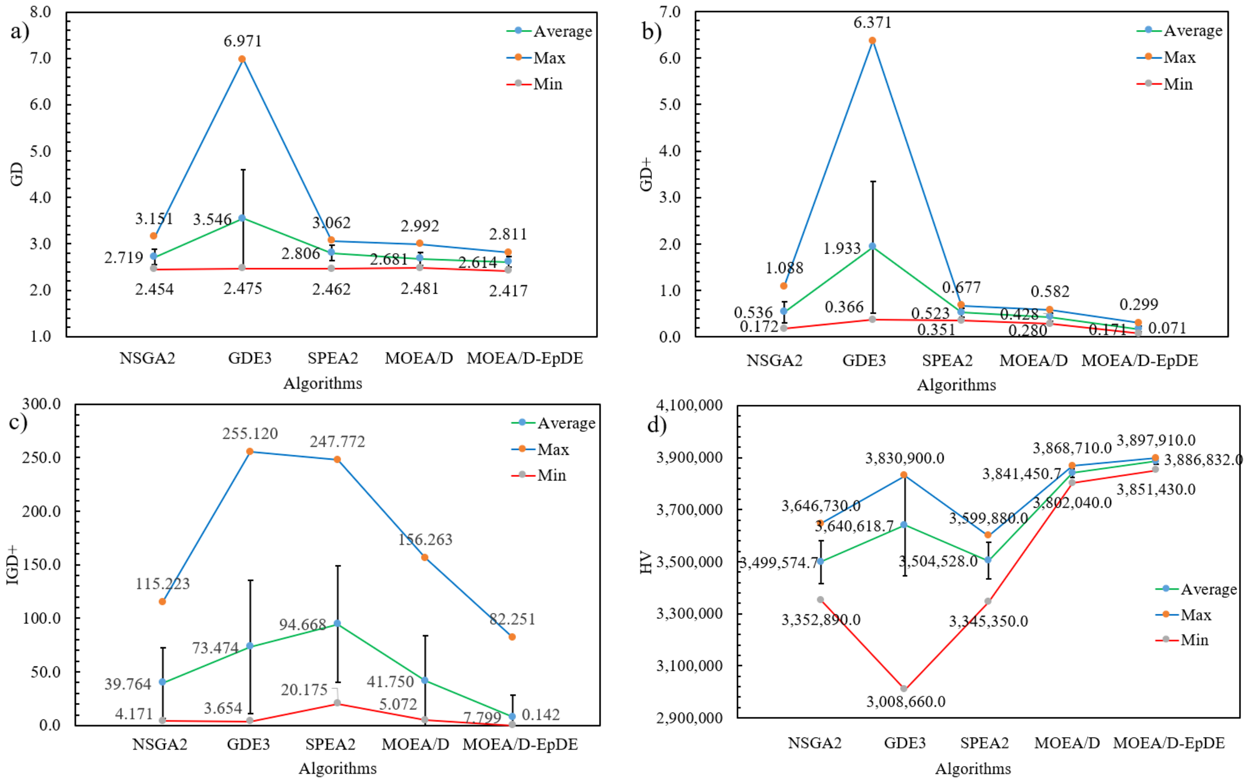

Figure 18. Performance indicators for 113-bar truss bridge: a) GD, b) GD+, c) IGD+, and d) HV

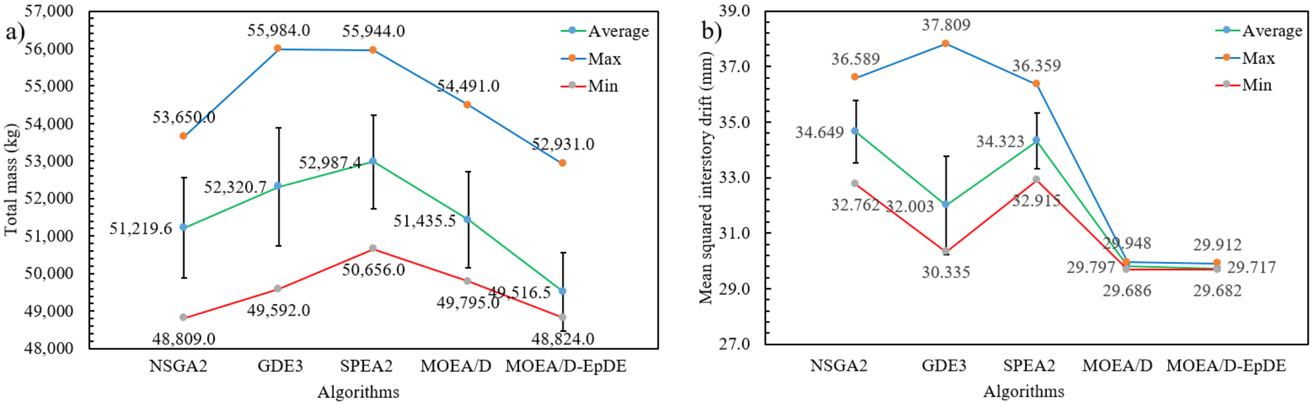

Figure 19. Anchor points for 113-bar truss bridge: a) First objective and b) Second objective

5. Conclusion

This study successfully evaluates the performance of MOMHs for truss MOO problems utilizing discrete design variables through direct analysis approaches. The primary focus of this research is on minimizing two conflicting objectives: the total mass of the structure and inter-story drift. Direct analysis is employed to rigorously evaluate constraints related to both strength and serviceability across various load combinations, ensuring that the design adheres to established safety and performance standards. To address these MOO challenges, five well-known and innovative MOO algorithms are utilized: NSGA2, GDE3, SPEA2, MOEA/D, and the novel MOEA/D-EpDE. The effectiveness of these algorithms is assessed on four popular truss structures, namely the 10-bar truss, 72-bar truss, 39-bar truss, and a 113-bar truss bridge. The results of the optimization reveal a nonlinear, inverse relationship between the two objectives, highlighting the inherent trade-offs involved in structural design decision-making.

The performance of each algorithm is evaluated using four key indicators: GD, GD+, IGD+, and HV, along with two anchor points. Notably, all algorithms successfully identified feasible solutions; however, MOEA/D-EpDE demonstrated superior performance by achieving the lowest values for GD, GD+, IGD+, and anchor points, as well as the highest HV values in the majority of scenarios. In terms of comparative performance, NSGA2 and MOEA/D surpassed GDE3 and SPEA2, indicating the effectiveness of the former algorithms in navigating the complexity of the MOO tasks. Looking ahead, prospective research should focus on the evaluation of additional algorithms to further deepen the understanding of MOO performance in the context of truss optimization. Moreover, several enhancements can be explored in future studies: (1) increasing the number of objectives beyond mass and inter-story drift to encompass other critical performance metrics, (2) investigating alternative structural systems, such as steel frames, which may present different optimization challenges, and (3) integrating complex loading scenarios, including fire and seismic forces, into the optimization framework. The authors are currently undertaking investigations into these aspects, which promise to refine and expand the scope of MOMHs in structural engineering applications. Ultimately, this study contributes valuable insights into the application of MOMHs for truss optimization, laying the groundwork for further advancements in this field.

6. Declarations

6.1. Author Contributions

Conceptualization, T.T. and Y.Y.; methodology, Q.V.; software, T.T.; formal analysis, T.T., Q.V., V.T., and N.N.; investigation, T.T.; data curation, T.T.; writing—original draft preparation, T.T. and Q.V.; writing—review and editing, V.T. and N.N.; supervision, V.T. and N.N.; project administration, N.N. All authors have read and agreed to the published version of the manuscript.

6.2. Data Availability Statement

Data sharing is not applicable to this article.

6.3. Funding

The authors received no financial support for the research, authorship, and/or publication of this article.

6.4. Conflicts of Interest

The authors declare no conflict of interest.

7. References

[1] Habibi, A. R., & Bidmeshki, S. (2018). A dual approach to perform geometrically nonlinear analysis of plane truss structures. Steel and Composite Structures, 27(1), 13–25. doi:10.12989/scs.2018.27.1.013.

[2] Thai, H. T., & Kim, S. E. (2009). Practical advanced analysis software for nonlinear inelastic analysis of space steel structures. Advances in Engineering Software, 40(9), 786–797. doi:10.1016/j.advengsoft.2009.02.001.

[3] Sheng-Xue, H. (2023). Truss optimization with frequency constraints using the medalist learning algorithm. Structures, 55, 1–15. doi:10.1016/j.istruc.2023.06.014.

[4] Ouardani, A. El, & Tbatou, T. (2024). Seismic Isolators Layout Optimization Using Genetic Algorithm Within the Pymoo Framework. Civil Engineering Journal (Iran), 10(8), 2517–2535. doi:10.28991/CEJ-2024-010-08-07.

[5] Altay, O., Cetindemir, O., & Aydogdu, I. (2024). Size optimization of planar truss systems using the modified salp swarm algorithm. Engineering Optimization, 56(4), 469–485. doi:10.1080/0305215X.2022.2160449.

[6] Kaveh, A., & Hosseini, S. M. (2022). Improved Bat Algorithm Based on Doppler Effect for Optimal Design of Special Truss Structures. Journal of Computing in Civil Engineering, 36(6), 4022028. doi:10.1061/(asce)cp.1943-5487.0001042.

[7] Nguyen, M. N., Hoang, V. N., & Lee, D. (2023). Multiscale topology optimization with stress, buckling and dynamic constraints using adaptive geometric components. Thin-Walled Structures, 183, 110405. doi:10.1016/j.tws.2022.110405.

[8] Yasin, A. A., Awwad, M. T., Malkawi, A. B., Maraqa, F. R., & Alomari, J. A. (2023). Optimization of Tuff Stones Content in Lightweight Concrete Using Artificial Neural Networks. Civil Engineering Journal (Iran), 9(11), 2823–2833. doi:10.28991/CEJ-2023-09-11-013.

[9] Contreras-Bejarano, O., & Villalba-Morales, J. D. (2024). On the use of the differential evolution algorithm for truss-type structures optimization. Applied Soft Computing, 161, 111372. doi:10.1016/j.asoc.2024.111372.

[10] Hajela, P., & Lee, E. (1995). Genetic algorithms in truss topological optimization. International Journal of Solids and Structures, 32(22), 3341–3357. doi:10.1016/0020-7683(94)00306-H.

[11] Bennage, W. A., & Dhingra, A. K. (1995). Optimization of truss topology using tabu search. International Journal for Numerical Methods in Engineering, 38(23), 4035–4052. doi:10.1002/nme.1620382308.

[12] Lamberti, L. (2008). An efficient simulated annealing algorithm for design optimization of truss structures. Computers & Structures, 86(19–20), 1936–1953. doi:10.1016/j.compstruc.2008.02.004.

[13] Serra, M., & Venini, P. (2006). On some applications of ant colony optimization metaheuristic to plane truss optimization. Structural and Multidisciplinary Optimization, 32(6), 499–506. doi:10.1007/s00158-006-0042-x.

[14] Schutte, J. F., & Groenwold, A. A. (2003). Sizing design of truss structures using particle swarms. Structural and Multidisciplinary Optimization, 25(4), 261–269. doi:10.1007/s00158-003-0316-5.

[15] Landa Becerra, R., & Coello, C. A. C. (2006). Cultured differential evolution for constrained optimization. Computer Methods in Applied Mechanics and Engineering, 195(33–36), 4303–4322. doi:10.1016/j.cma.2005.09.006.

[16] Degertekin, S. O., Lamberti, L., & Ugur, I. B. (2018). Sizing, layout and topology design optimization of truss structures using the Jaya algorithm. Applied Soft Computing Journal, 70, 903–928. doi:10.1016/j.asoc.2017.10.001.

[17] Pierezan, J., dos Santos Coelho, L., Cocco Mariani, V., Hochsteiner de Vasconcelos Segundo, E., & Prayogo, D. (2021). Chaotic coyote algorithm applied to truss optimization problems. Computers & Structures, 242, 106353. doi:10.1016/j.compstruc.2020.106353.

[18] Kaveh, A., & Mahdavi, V. R. (2015). Colliding bodies optimization for size and topology optimization of truss structures. Structural Engineering and Mechanics, 53(5), 847–865. doi:10.12989/sem.2015.53.5.847.

[19] Madah, H., & Amir, O. (2017). Truss optimization with buckling considerations using geometrically nonlinear beam modeling. Computers & Structures, 192, 233–247. doi:10.1016/j.compstruc.2017.07.023.

[20] Missoum, S., Gürdal, Z., & Gu, W. (2002). Optimization of nonlinear trusses using a displacement-based approach. Structural and Multidisciplinary Optimization, 23(3), 214–221. doi:10.1007/s00158-002-0179-1.

[21] Hrinda, G. A., & Nguyen, D. T. (2008). Optimization of stability-constrained geometrically nonlinear shallow trusses using an arc length sparse method with a strain energy density approach. Finite Elements in Analysis and Design, 44(15), 933–950. doi:10.1016/j.finel.2008.07.004.

[22] Kameshki, E. S., & Saka, M. P. (2007). Optimum geometry design of nonlinear braced domes using genetic algorithm. Computers and Structures, 85(1–2), 71–79. doi:10.1016/j.compstruc.2006.09.002.

[23] Martinez, S. Z., & Coello, C. A. C. (2014). A multi-objective evolutionary algorithm based on decomposition for constrained multi-objective optimization. IEEE Congress on Evolutionary Computation (CEC), 429–436. doi:10.1109/cec.2014.6900645.

[24] Deb, K., Agrawal, S., Pratap, A., Meyarivan, T. (2000). A Fast Elitist Non-dominated Sorting Genetic Algorithm for Multi-objective Optimization: NSGA-II. Parallel Problem Solving from Nature PPSN VI, PPSN 2000. Lecture Notes in Computer Science, 1917. Springer, Berlin, Germany. doi:10.1007/3-540-45356-3_83.

[25] Sarker, R., Liang, K. H., & Newton, C. (2002). A new multiobjective evolutionary algorithm. European Journal of Operational Research, 140(1), 12–23. doi:10.1016/S0377-2217(01)00190-4.

[26] Kukkonen, S., & Lampinen, J. (2005). GDE3: The third Evolution Step of Generalized Differential Evolution. 2005 IEEE Congress on Evolutionary Computation, 1, 443–450. doi:10.1109/cec.2005.1554717.

[27] Gholizadeh, S., & Fattahi, F. (2021). Multi-objective design optimization of steel moment frames considering seismic collapse safety. Engineering with Computers, 37(2), 1315–1328. doi:10.1007/s00366-019-00886-y.

[28] Eid, H. F., Garcia-Hernandez, L., & Abraham, A. (2022). Spiral water cycle algorithm for solving multi-objective optimization and truss optimization problems. Engineering with Computers, 38, 963–973. doi:10.1007/s00366-020-01237-y.

[29] Kaveh, A., & Ilchi Ghazaan, M. (2020). A new VPS-based algorithm for multi-objective optimization problems. Engineering with Computers, 36(3), 1029–1040. doi:10.1007/s00366-019-00747-8.

[30] Lemonge, A. C. C., Carvalho, J. P. G., Hallak, P. H., & Vargas, D. E. C. (2021). Multi-objective truss structural optimization considering natural frequencies of vibration and global stability. Expert Systems with Applications, 165, 113777. doi:10.1016/j.eswa.2020.113777.

[31] Ho-Huu, V., Duong-Gia, D., Vo-Duy, T., Le-Duc, T., & Nguyen-Thoi, T. (2018). An efficient combination of multi-objective evolutionary optimization and reliability analysis for reliability-based design optimization of truss structures. Expert Systems with Applications, 102, 262–272. doi:10.1016/j.eswa.2018.02.040.

[32] Cao, T. S., Pham, H. A., & Truong, V. H. (2024). An efficient algorithm for multi-objective structural optimization problems using an improved pbest-based differential evolution algorithm. Advances in Engineering Software, 197, 103752. doi:10.1016/j.advengsoft.2024.103752.

[33] Cao, T. S., Nguyen, T. T. T., Nguyen, V. S., Truong, V. H., & Nguyen, H. H. (2023). Performance of Six Metaheuristic Algorithms for Multi-Objective Optimization of Nonlinear Inelastic Steel Trusses. Buildings, 13(4), 868. doi:10.3390/buildings13040868.

[34] Panagant, N., Pholdee, N., Bureerat, S., Yildiz, A. R., & Mirjalili, S. (2021). A Comparative Study of Recent Multi-objective Metaheuristics for Solving Constrained Truss Optimisation Problems. Archives of Computational Methods in Engineering, 28(5), 4031–4047. doi:10.1007/s11831-021-09531-8.

[35] Panagant, N., Kumar, S., Tejani, G. G., Pholdee, N., & Bureerat, S. (2023). Many‐objective meta-heuristic methods for solving constrained truss optimisation problems: A comparative analysis. MethodsX, 10, 102181. doi:10.1016/j.mex.2023.102181.

[36] Nguyen, H. H., & Truong, V. H. (2024). Machine Learning-based prediction of seismic lateral deflection of steel trusses using nonlinear time-history analysis. Structures, 69, 107369. doi:10.1016/j.istruc.2024.107369.

[37] Truong, V. H., Tangaramvong, S., & Papazafeiropoulos, G. (2024). An efficient LightGBM-based differential evolution method for nonlinear inelastic truss optimization. Expert Systems with Applications, 237, 121530. doi:10.1016/j.eswa.2023.121530.

[38] Nguyen, Q.-B. (2024). An Efficient Framework for Optimization of Nonlinear Steel Trusses with Continuous Variables Using Lightgbm. International Journal of Geomate, 26(116). doi:10.21660/2024.116.4398.

[39] Blandford, G. E. (1996). Progressive failure analysis of inelastic space truss structures. Computers and Structures, 58(5), 981–990. doi:10.1016/0045-7949(95)00217-5.

[40] Yang, Y.-B., & Kuo, S.-R. (1994). Theory & Analysis of Nonlinear Framed Structures. Prentice Hall. Hoboken, United States.

[41] Yang, Y. Bin, & Shieh, M. S. (1990). Solution method for nonlinear problems with multiple critical points. AIAA Journal, 28(12), 2110–2116. doi:10.2514/3.10529.

[42] Srinivas, N., & Deb, K. (1994). Muiltiobjective Optimization Using Nondominated Sorting in Genetic Algorithms. Evolutionary Computation, 2(3), 221–248. doi:10.1162/evco.1994.2.3.221.

[43] Deb, K., & Agrawal, R. B. (1995). Simulated binary crossover for continuous search space. Complex systems, 9(2), 115-148.

[44] Zitzler, E., & Thiele, L. (1999). Multiobjective evolutionary algorithms: A comparative case study and the strength Pareto approach. IEEE Transactions on Evolutionary Computation, 3(4), 257–271. doi:10.1109/4235.797969.

[45] Zitzler, E., Laumanns, M., Thiele, L., et al. (2001). SPEA2: Improving the strength Pareto evolutionary algorithm. TIK Report, Computer Engineering and Networks Laboratory, ETH Zurich, Zürich, Switzerland. doi:10.3929/ethz-a-004284029.

[46] Zhang, Q., & Li, H. (2007). MOEA/D: A multiobjective evolutionary algorithm based on decomposition. IEEE Transactions on Evolutionary Computation, 11(6), 712–731. doi:10.1109/TEVC.2007.892759.